PNAS RESEARCH ARTICLE | GENETICS

# Loss of the endoplasmic reticulum protein Tmem208 affects cell polarity, development, and viability

Debdeep Dutta[a,b], Oguz Kanca[a,b], Rishi V. Shridharan[a,b], Paul C. Marcogliese[a,b,1], Benjamin Steger[c], Marie Morimoto[c], F. Graeme Frost[c], Ellen Macnamara[c], Undiagnosed Diseases Network[2], Michael F. Wangler[a,b], Shinya Yamamoto[a,b], Andreas Jenny[d,e], David Adams[c], May C. Malicdan[c], and Hugo J. Bellen[a,b,3]

Contributed by Hugo J. Bellen; received December 29, 2023; accepted January 26, 2024; reviewed by Marek Mlodzik and Hyung Don Ryoo

**Nascent proteins destined for the cell membrane and the secretory pathway are targeted to the endoplasmic reticulum (ER) either posttranslationally or cotranslationally. The signal-independent pathway, containing the protein TMEM208, is one of three pathways that facilitates the translocation of nascent proteins into the ER. The in vivo function of this protein is ill characterized in multicellular organisms. Here, we generated a CRISPR-induced null allele of the fruit fly ortholog *CG8320/Tmem208* by replacing the gene with the *Kozak-GAL4* sequence. We show that *Tmem208* is broadly expressed in flies and that its loss causes lethality, although a few short-lived flies eclose. These animals exhibit wing and eye developmental defects consistent with impaired cell polarity and display mild ER stress. Tmem208 physically interacts with Frizzled (Fz), a planar cell polarity (PCP) receptor, and is required to maintain proper levels of Fz. Moreover, we identified a child with compound heterozygous variants in *TMEM208* who presents with developmental delay, skeletal abnormalities, multiple hair whorls, cardiac, and neurological issues, symptoms that are associated with PCP defects in mice and humans. Additionally, fibroblasts of the proband display mild ER stress. Expression of the reference human *TMEM208* in flies fully rescues the loss of *Tmem208*, and the two proband-specific variants fail to rescue, suggesting that they are loss-of-function alleles. In summary, our study uncovers a role of TMEM208 in development, shedding light on its significance in ER homeostasis and cell polarity.**

TMEM proteins | hSnd2 | PCP | ER stress | *Drosophila*

## Significance

The biological significance of *TMEM208* is unknown in multicellular organisms. We show that loss of *Tmem208*, the fly ortholog of human *TMEM208*, results in lethality, and escapers exhibit defects in the wing and eye indicative of a disruption in planar cell polarity (PCP). Tmem208 binds the PCP receptor Frizzled and helps maintain its proper levels. An individual who carries biallelic loss-of-function alleles of *TMEM208* presents with developmental delay and a multisystem disorder consistent with PCP defects.

TMEM (**T**rans**MEM**brane) proteins are present in the cell membrane as well as other membrane-bound organelles including the nucleus, mitochondria, lysosome, and endoplasmic reticulum (ER). In humans, the TMEM protein family consists of over 300 members, many of which have been associated with cancer, neurodegeneration, and a range of genetic disorders (1–10). Many of these TMEM proteins are localized to the ER. Despite their abundance, the functional importance of these ER-localized TMEM proteins in multicellular organisms remains poorly characterized. To gain insight into the role of ER-resident TMEM proteins in development, in this study, we conducted an RNA interference (RNAi) screen targeting conserved ER-resident TMEM proteins in fruit flies. This screen revealed that many genes encoding ER-localized TMEM proteins are essential for fruit fly (*Drosophila melanogaster*) development. Through the Undiagnosed Diseases Network (UDN), we identified an individual with compound heterozygous variants in *TMEM208* who presents with developmental delay, dysmorphism, multiple hair whorls, seizures, and other developmental abnormalities involving multiple organs. These data prompted us to assess the role of this gene in development in more detail using fruit flies to establish a human disease model. Based on experiments in yeast and human cell lines, TMEM208 has been implicated in the transport of nascent polypeptides into the ER via the signal recognition particle (SRP)-independent (SND) pathway (11, 12). Proteins destined for the cell membrane, endomembrane system, and secretory pathway are first targeted to the ER before they are sent to their destination. Proteins with an N-terminal signal peptide and/or transmembrane domain are transported to the ER cotranslationally via another pathway, the SRP pathway (13, 14). However, proteins with a C-terminal transmembrane domain are transported to the ER posttranscriptionally via the Guided Entry of Tail (GET) pathway (13, 14). The Snd2 protein in yeast, the ortholog of human TMEM208/hSnd2, was discovered as a component of the SND pathway which shows a preference toward proteins with an internal transmembrane domain (11). Genetic experiments in yeast suggest that the SND pathway acts as a backup for the other two pathways and that some proteins can use SND and SRP/GET pathways (*SI Appendix*, Fig. S1*A*). Based on experiments in human cell lines, the SND pathway was shown to be dependent

Author affiliations: [a]Department of Molecular and Human Genetics, Baylor College of Medicine, Houston, TX 77030; [b]Jan and Dan Duncan Neurological Research Institute, Texas Children's Hospital, Houston, TX 77030; [c]NIH Undiagnosed Diseases Program, National Human Genome Research Institute, NIH, Bethesda, MD 20892; [d]Department of Developmental and Molecular Biology, Albert Einstein College of Medicine, New York, NY 10461; and [e]Department of Genetics, Albert Einstein College of Medicine, New York, NY 10461

Author contributions: D.D., U.D.N., and H.J.B. designed research; D.D., O.K., R.V.S., P.C.M., B.S., M.M., F.G.F., E.M., U.D.N., M.F.W., S.Y., A.J., D.A., M.C.M., and H.J.B. performed research; O.K., P.C.M., and H.J.B. contributed new reagents/analytic tools; D.D., R.V.S., B.S., M.M., F.G.F., E.M., A.J., M.C.M., and H.J.B. analyzed data; and D.D., O.K., R.V.S., P.C.M., B.S., M.M., F.G.F., E.M., S.Y., A.J., M.C.M., and H.J.B. wrote the paper.

Reviewers: M.M., Icahn School of Medicine at Mount Sinai; and H.D.R., New York University School of Medicine.

The authors declare no competing interest.



[1]Present address: Department of Biochemistry & Medical Genetics, University of Manitoba, Winnipeg, MB, CA R3E 0J9.

[2]A complete list of the Undiagnosed Diseases Network can be found in the *SI Appendix*.

[3]To whom correspondence may be addressed. Email: hbellen@bcm.edu.

This article contains supporting information online at https://www.pnas.org/lookup/suppl/doi:10.1073/pnas.2322582121/-/DCSupplemental.

Published February 21, 2024.

on TMEM208 (12, 15). However, the phenotypes associated with loss of TMEM208 in multicellular organisms have not yet been established.

To study the functional consequences of *Tmem208* loss, we generated a fly mutant, assessed the expression pattern of this gene, and characterized the loss-of-function phenotypes. We also generated a GFP-tagged *Tmem208* allele to determine the subcellular localization of the Tmem208 protein. Loss of the gene results in lethality with few escapers exhibiting reduced lifespan, neurological issues, some planar cell polarity (PCP) defects, as well as other developmental defects. A human *TMEM208* transgene rescues the lethality of the mutants, indicating functional conservation. Loss of *Tmem208* also induces a mild ER stress. Furthermore, our data revealed that Tmem208 interacts with Frizzled (Fz), a component of the PCP pathway, and helps to maintain proper levels of Fz. Using the humanized fly models, we demonstrated that the variants identified in a UDN subject are loss-of-function alleles. Altogether, our findings show that *Tmem208* and *TMEM208* are evolutionarily conserved players in multicellular development, and their loss results in multisystem defects.

## Results

**ER-Resident TMEM Proteins Are Important for Fruit Fly Development.** In an attempt to identify the possible subcellular localization of ~300 human TMEM proteins (www.uniprot.org), we performed a literature survey. This revealed that a significant fraction (n > 60) of human TMEM proteins are localized to the ER membrane, and ~70% of the human ER-resident TMEM protein-encoding genes have at least one ortholog in flies, and ~60% of these are highly conserved (Drosophila RNAi Screening Center Integrative Ortholog Prediction Tool (DIOPT) score ≥7/15) (16). To evaluate the role of the highly conserved ER proteins in development, we targeted 38 *TMEM* genes in an RNAi screen. We performed either a ubiquitous knockdown [*Tubulin(Tub)-GAL4*] or a wing-specific knockdown [*nubbin(nub)-GAL4*] that drives expression in the pouch region of the larval wing disc using the UAS-GAL4 system (17). Thirty RNAis caused a partial or complete lethality upon ubiquitous gene knockdown and 12 of the 38 genes caused a phenotype upon wing-specific gene knockdown. Eleven of the RNAi lines cause both lethality and a wing phenotype (*SI Appendix*, Table S1). In some instances, such as the knockdown of *CG14646* (ortholog of human *TMEM129*) and *CG30389* (ortholog of human *TMEM57*), wing-specific knockdown resulted in severely affected wings (*SI Appendix*, Fig. S1*B*). In other instances, RNAi-mediated knockdown resulted in a spectrum of phenotypes including wing notching, blistering, wing vein and crossvein malformation, as well as crumpled wings (*SI Appendix*, Fig. S1*B*).

One of the candidates identified in the screen was *CG8320* an as yet-uncharacterized fly ortholog of human *TMEM208.* The corresponding human and fly proteins share 43% identity and 65% similarity in amino acid composition (DIOPT score 14/15) as well as a similar topology (*SI Appendix*, Fig. S1 *C* and *D*). Specifically, ubiquitous knockdown of *Tmem208* results in lethality while wing knockdown produces blisters, crossvein formation defects, and PCP-like defects. The latter phenotype drew our interest as the UDN identified an individual with compound heterozygous variants in *TMEM208.* To interrogate the relevance of those *TMEM208* variants, we sought to further characterize the function of this gene in flies.

***Tmem208* Is Broadly Expressed, and Its Loss Causes Lethality.** To evaluate the role of *Tmem208* in development, we generated a knockout allele, $Tmem208^{KG4}$, using CRISPR-induced homologous recombination (18). Two guide RNAs targeting the 5′ and 3′Untranslated Region (UTRs) of the endogenous gene along with the donor plasmid with left and right homology arms were used to replace the entire open reading frame of *Tmem208* with a *Kozak-GAL4* (*GAL4* with a Kozak sequence for efficient translation) sequence (Fig. 1*A*). This allele expresses the *GAL4* gene under the endogenous promoter of *Tmem208*. We used this allele to drive nuclear-localized reporter transgene *UAS-mCherry.NLS* (nuclear localized fluorescent protein) and examined the expression pattern at different developmental stages (19, 20). The gene is expressed in larval, pupal, and adult stages in fruit flies (Fig. 1*B*). In the 3rd instar larvae, *Tmem208* is broadly expressed in almost all tissues including wing disc, leg disc, eye disc, brain, salivary gland, anterior gut, fat body, and Malpighian tubules (Fig. 1*C*). We also noted expression of *Tmem208* in the adult fly brain (*SI Appendix*, Fig. S2*A*). To identify the specific cell populations in the brain that express *Tmem208*, we used $Tmem208^{KG4}$> *UAS-mCherry.NLS* flies and performed costaining against mCherry and either Elav (Embryonic lethal abnormal vision), a pan-neuronal protein, or Repo (Reversed polarity), a glial protein (21). As shown in *SI Appendix*, Fig. S2*A*, *Tmem208* is expressed in subsets of neurons and glia of the adult brain.

The $Tmem208^{KG4}$ allele results in semilethality with ~10% escapers when tested in heterozygous flies carrying one of two molecularly defined deficiencies (*Df*), (*Df(2R)Exel7138/CyO* and *Df(2R)BSC308/CyO*). Quantitative RT-PCR data revealed no transcript in $Tmem208^{KG4}$/(*Df(2R)Exel7138* animals (Fig. 1*D*). Escapers display a significantly reduced life span when compared to control flies (*SI Appendix*, Fig. S2*B*). The lethality associated with the *Tmem208* mutants is fully rescued by introducing a genomic rescue (GR) construct (22) that contains a copy of the *Tmem208* gene (Fig. 1 *E* and *F*). In summary, *Tmem208* is broadly expressed, important for survival, and escapers have a reduced lifespan.

***Tmem208* Mutants Display Cell Polarity Defects.** In addition to the reduced lifespan, $Tmem208^{KG4}$/*Df* mutant escapers displayed a spectrum of morphological defects. For example, in 29.6% of the escapers (n = 140), we observed a defect in tarsal development (kinked segment) (*SI Appendix*, Fig. S2*C*). We also noted morphological anomalies in eye and wing tissues. Retinal sections revealed a variety of subtle defects. The fly eye consists of ~800 units called ommatidium. Each ommatidium typically consists of eight photoreceptor (PR) neurons (R1-R8) with each having a prominent rhabdomere that plays a critical role in phototransduction. Six of the PRs rhabdomeres (R1 to R6) are peripheral, whereas two PRs rhabdomeres (R7 and R8) are central (23). The R7 and R8 PR are on top of each other, and only seven PR/rhabdomeres are visible in each section (Fig. 2*A*). In some mutant ommatidia, we observe rhabdomere loss, whereas in other ommatidia, there are more than seven rhabdomeres as well as elongated rhabdomeres (Fig. 2 *B* and *B'*). Additionally, in several instances, we observe a "supernumerary PR", a cell that looks like another R3 PR leading to an M shape of the PR organization rather than a trapezoidal shape (Fig. 2*B*). We also noticed a mild PCP defect-like phenotype with miss-rotated ommatidia (Fig. 2 *A'* and *B'*). Transmission electron microscopy (TEM) demonstrates that the extra-rhabdomere phenotype is due to the presence of two rhabdomeres in the same PR (Fig. 2 *A"* and *B"*). This defect appears to be an apical–basal polarity defect (24–27). During development, apicobasal polarity is established in the PR cells, and the apical membrane then reorganizes to form the stalk and rhabdomeres (28). Loss of proteins that establish apicobasal polarity during rhabdomere formation can cause similar phenotypes as those shown in Fig. 2 *B* and *B"*. In sum, these data suggest that loss of *Tmem208* causes mild cell polarity defects in the fly eye.

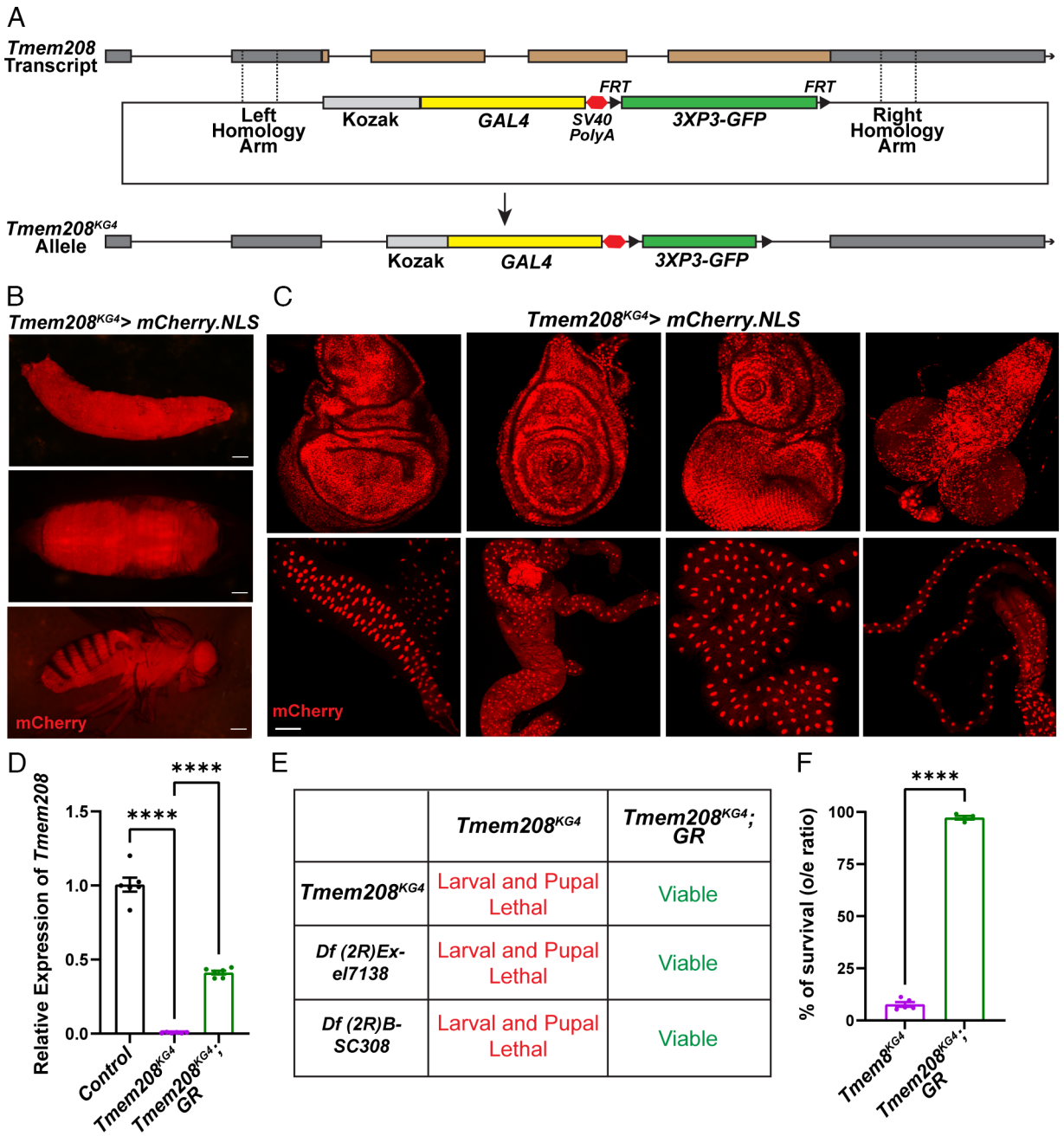


**Fig. 1.** CG8320/*Tmem208* is a broadly expressed gene essential for survival. (*A*) Generation strategy of *Tmem208*$^{KG4}$ allele. (*B*) Expression of *Tmem208*$^{KG4}$-driven mCherry.NLS at different stages of the fly lifecycle. (*C*) Expression of *Tmem208*$^{KG4}$-driven mCherry.NLS in different larval tissues. *Upper* panel (from *Left* to *Right*): wing disc, leg disc, eye disc, and larval brain; *Lower* panel (from *Left* to *Right*): salivary gland, anterior gut, fat body, and Malpighian tubule. Scale bar: 100 μm. (*D*) *Tmem208* transcripts are undetectable in *Tmem208*$^{KG4}$ mutants. (*E* and *F*) *Tmem208*$^{KG4}$is a strong loss-of-function allele that is complemented by introduction of one copy of a P[acman] genomic rescue (GR) construct (22). To determine the statistical significance between two genotypes, a two-tailed Student's *t* test was used. To determine the statistical significance between three genotypes, one-way ANOVA followed by a Tukey's post hoc test was used. Error bars represent SEM (****$P < 0.0001$).

We also observed wing defects in escapers. Some of the escapers (31.4%, n = 86) exhibit anterior crossvein formation defects (Fig. 2 *C* and *D*). In addition, 13.2% (n = 53) of the escapers display improper wing folding (Fig. 2*E*), and ~10% of escapers display locally misaligned wing hairs, a phenotype reminiscent of PCP or PCP effector defects (Fig. 2 *C'–F*). Hence, the data again suggests that loss of *Tmem208* causes a PCP-like phenotype in eye and wing with incomplete penetrance.

***Tmem208* Encodes an ER-Resident Protein, and Its Loss Induces Mild ER Stress.** To assess the subcellular localization of Tmem208 protein in vivo, we generated a *Tmem208-GFP* allele. A Green Fluorescent Protein (GFP) sequence, along with linker sequences, was inserted in *Tmem208* (between amino acids R99 and E100) using CRISPR-mediated homologous recombination (Fig. 3*A*) (18). The resulting allele produced an internally GFP-tagged Tmem208 protein. Animals carrying the *Tmem208-GFP* allele in homozygous condition or in trans with the *Tmem208*$^{KG4}$ allele are lethal. However, introducing one copy of GR rescued the lethality associated with this allele (*SI Appendix*, Fig. S3*A*), indicating that it is a loss-of-function allele. We used the salivary gland and fat body from heterozygous *Tmem208-GFP* larva and performed immunostaining for GFP to assess the protein localization and costained for Calnexin, an ER marker. As shown in Fig. 3*B* and *SI Appendix*, Fig. S3*B*, GFP and Calnexin colocalize in the ER indicating that Tmem208-GFP is properly localized.

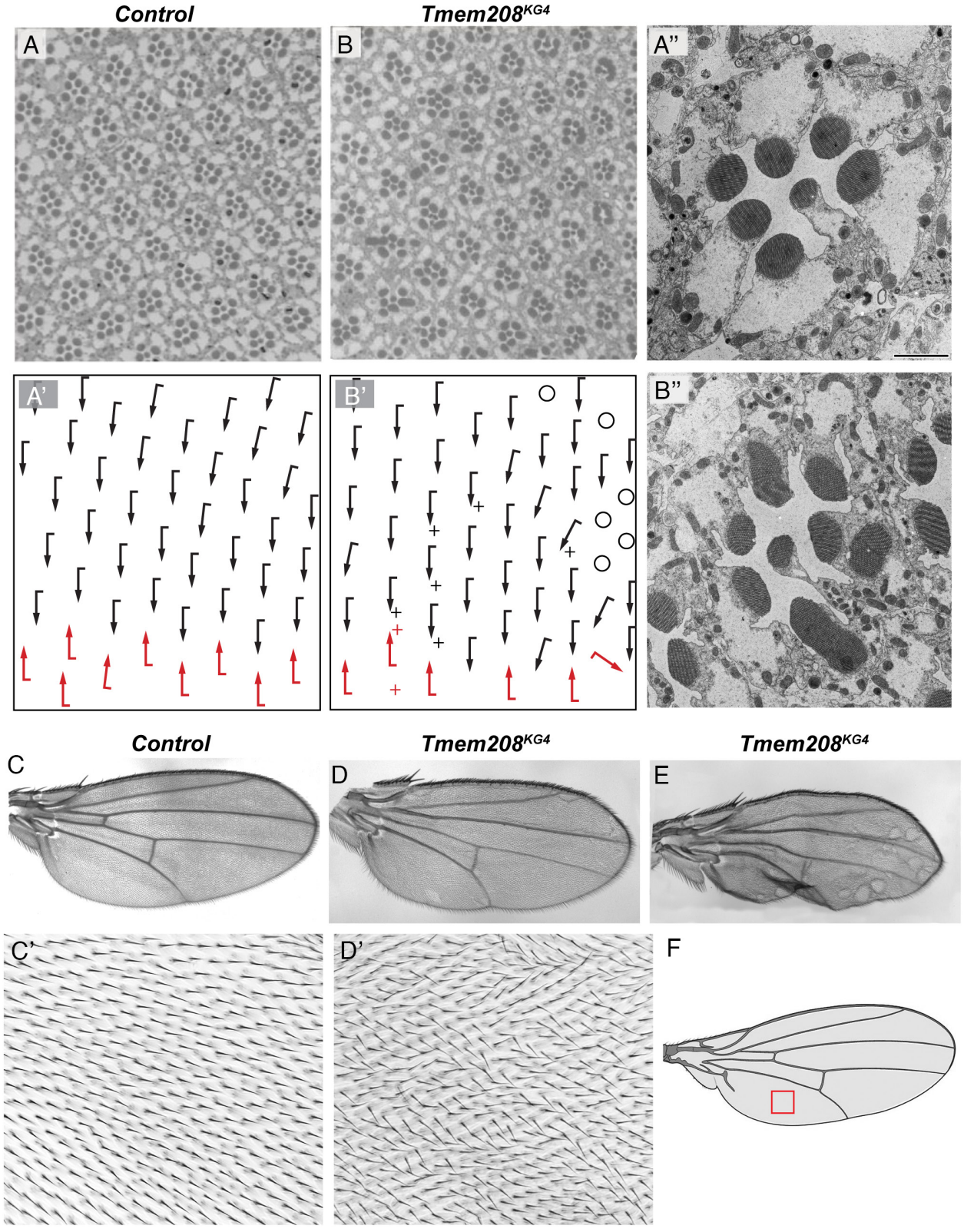


**Fig. 2.** Loss of *Tmem208* causes developmental defects and impairs cell polarity. (*A* and *B*) Retinal images of control and escaper mutant flies. (*A'* and *B'*) Arrow diagram showing the polarity of each ommatidium in the retina. "o" indicates missing rhabdomere and "+" indicates extra rhabdomere. Black and Red arrows indicate Dorsal and Ventral chirality. (*A''* and *B''*) TEM images of single ommatidia from the control (*Upper*) and mutant (*Lower*) animals. Scale bar: 2 μm. (*C*–*E*) Wing images from control and two *Tmem208* escaper mutant flies. (*C'* and *D'*) Higher magnification images from wing from control (*Left*) and mutant (*Right*) showing the orientation of wing bristles. (*F*) The area in the red box indicates the region used for the images shown in *C'* and *D'*. The wing image in *F* was drawn using Biorender.

Next, we explored the cellular consequences of loss of *Tmem208*. An earlier study reported increased ER stress upon knockdown of *TMEM208* in human U2OS epithelial-like cell lines (29). We therefore evaluated the levels of different ER stress markers in *Tmem208* mutants by performing western blot and/or immunocytochemistry for the ER stress markers. When unfolded proteins

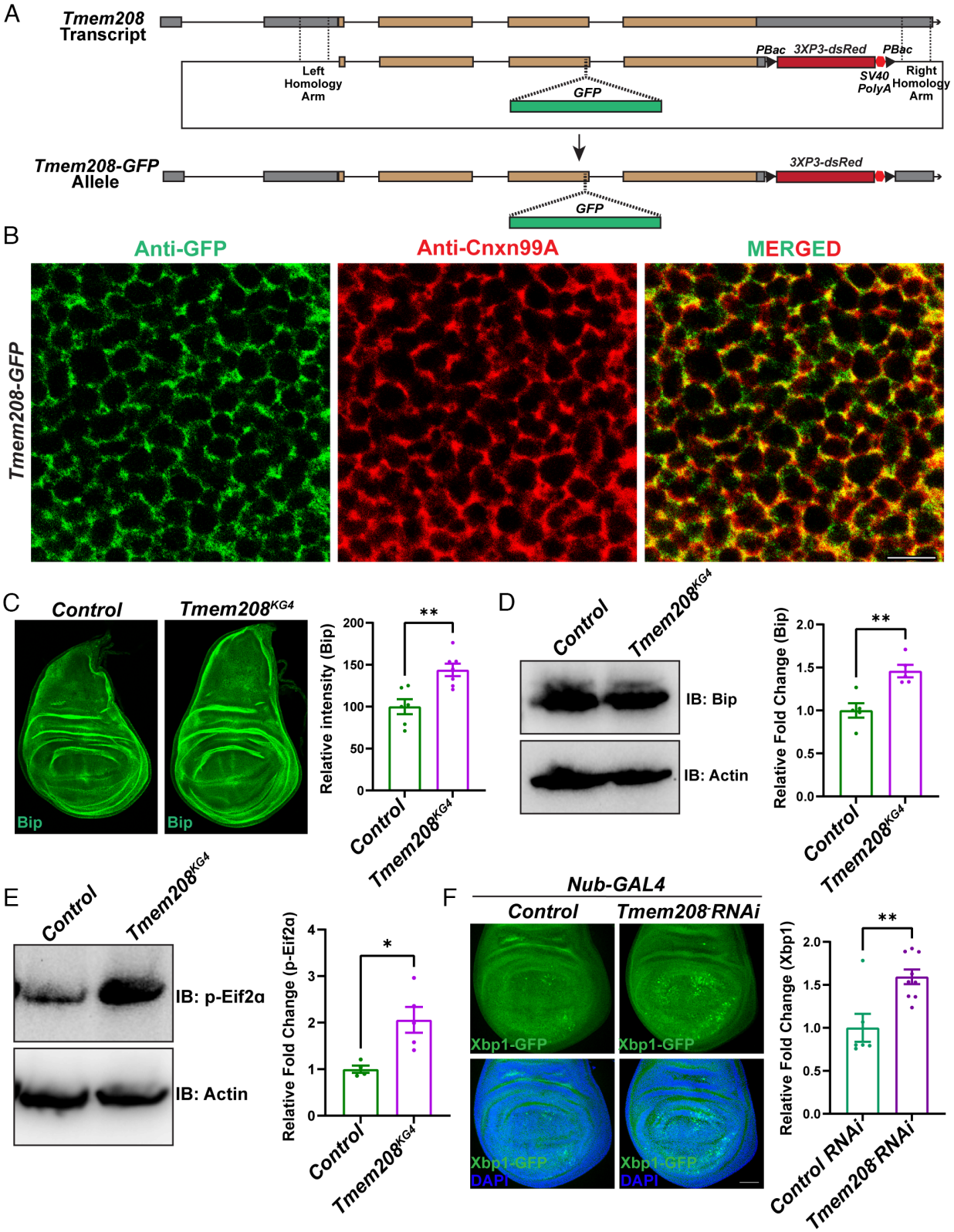


**Fig. 3.** *Tmem208* encodes an endoplasmic-reticulum resident protein, and its loss causes mild ER stress. (*A*) Nature of the *Tmem208-GFP* allele. (*B*) Colocalization of Tmem208-GFP and calnexin proteins in the salivary gland. Scale bar: 5 μm. (*C*) Control and mutant wing discs with Bip/GRP78 staining and its quantification. (*D*) Western blot and quantification showing relative Bip/GRP78 protein levels in $Tmem208^{KG4}$ mutants. (*E*) Western blot and quantification showing relative p-Eif2α protein levels in $Tmem208^{KG4}$ mutants. (*F*) Anti-GFP (for detecting Xbp1-GFP protein) staining in the pouch area of the wing disc from the animals of the indicated genotype and related quantification. Scale bar: 50 μm. The fold changes in the experimental samples are relative to the control samples. To determine the statistical significance between two genotypes, two-tailed Student's *t* test was used. Error bars represent SEM (*$P < 0.05$; **$P < 0.01$).

accumulate in the ER lumen, Bip (encoded by *Hsc70-3*, the fly ortholog of human *HSPA5*/*GRP78*) senses these proteins and initiates an ER stress response (30–32). We measured the Bip protein level in $Tmem208^{KG4}$ mutants using two different approaches: First, we performed immunostaining using the anti-Bip antibody in the wing discs of $Tmem208^{KG4}/Df$ larvae;

second, we performed western blot analyses to detect the Bip protein levels in these mutants. As shown in Fig. 3 *C* and *D*, a ~1.5-fold increase in the Bip protein levels was observed in both wing discs as well as in mutants. Subsequent signaling cascades lead to the phosphorylation of Eif2α and repression of the translational machinery (30, 33). Consistent with this, the p-Eif2α protein levels were elevated in *Tmem208* mutants when compared to controls (Fig. 3*E*). Finally, upon initiation of ER stress, alternative splicing allows for the expression of Xbp1 (32, 34, 35). We measured the levels of Xbp1 upon RNAi-mediated knockdown of *Tmem208* using a transgene in which Xbp1 is located upstream of a GFP construct. In this reporter line, ER stress induces Xbp1 mRNA splicing leading to the expression of Xbp1-GFP (32, 35). As shown in Fig. 3*F*, an increase in the GFP levels is observed in the pouch region of 3rd instar larval wing discs upon knockdown of *Tmem208*. Taken together, these data indicate that loss of *Tmem208* causes a modest but consistent ER stress response.

**Tmem208 Helps to Maintain Fz Protein Levels.** Since *Tmem208* null mutants displayed a PCP-like phenotype and Fz-signaling regulates establishing PCP, we subsequently tested whether Tmem208 interacts with Fz. PCP orients cells to create a polarity within tissue. Several of the proteins in this pathway are transmembrane membrane proteins (36) and are imported into the ER prior to being transported to the cell membrane. In the classical Fz-signaling pathway, six proteins are involved (36, 37). Three of these proteins (Prickle, Diego, and Dishevelled) do not have a transmembrane (TM) domain, whereas the other three proteins (Fz, Van Gogh, and Starry night/Flamingo) contain C-terminal or internal TM domains, suggesting that Tmem208 may play a role in facilitating the transport of these latter proteins. To assess this possibility, we tested whether Fz interacts directly with Tmem208 using immunoprecipitation (IP). We ubiquitously overexpressed HA-tagged Tmem208 and performed IP using anti-HA antibody, followed by western blot analysis targeting against Fz. Our results showed that endogenous Fz indeed immunoprecipitated with Tmem208 (Fig. 4*A*), providing evidence that these two proteins interact.

Next, we measured the effects of *Tmem208* loss on Fz protein levels using western blotting. As shown in Fig. 4 *B* and *C*, Fz protein levels are reduced in $Tmem208^{KG4}/Df$ escaper flies. In addition, we performed immunostaining in the larval wing disc to detect the levels of Fz protein. However, we were not able to detect endogenous Fz protein in the 3rd instar larval wing discs. We therefore overexpressed Fz either in a wild-type background or in a *Tmem208-GFP* mutant heterozygous background and consistently observed decreased Fz protein levels in the wing discs of *Tmem208-GFP* heterozygous larva (Fig. 4 *D* and *E*). Taken together, our data indicate that Tmem208 interacts with Fz and plays a role in maintaining proper Fz protein levels.

**Biallelic Variants in *TMEM208* Are Associated with Developmental Defects in Humans.** Through the UDN, we identified a 5-y-old child with global developmental delay and a multisystemic disorder (*SI Appendix*, Fig. S4*A*). The individual was born with neonatal respiratory distress, gut malrotation, and dysmorphic features. Additionally, the subject has abnormal skeletal and ocular features, lymphopenia, and heart defects. Other features included failure to thrive, perioral cyanosis with feeding, seizures, idiopathic intracranial hypertension with papilledema, hypoglycemia, idiopathic dilatation of the main pulmonary artery and aortic root, two posterior parietal hair whorls, frontal prominence, bilateral epicanthal folds, micrognathia, short neck, and a mild 5th finger clinodactyly (see *SI Appendix, Supplementary Clinical Information*, for more detail). Genome sequencing revealed compound heterozygous variants in *TMEM208* (NM_014187.3) (*SI Appendix*, Fig. S4*B*). The first variant (NM_014187.3: c.80T>C, p.L27P) is a point mutation (Fig. 5*A*) and the CADD score is 25.1 (38). This allele is present *in trans* to a frameshift variant (NM_014187.3: c.177delT, p.F59fs*13) (Fig. 5*A*) that likely leads to the production of a truncated TMEM208 protein (predicted to be truncated in the middle of the second transmembrane domain) or the absence of protein because of nonsense-mediated decay.

We assessed the nature of the *TMEM208* variants identified in the UDN subject using a "humanized" fruit fly model. As shown in Fig. 5*B*, loss of *Tmem208* causes lethality in fruit flies, and expression of the human *TMEM208* reference transgene rescues the lethality of these mutants. In contrast, expression of the transgene encoding the p.L27P variant only partially rescued the lethality, whereas the p.F59Lfs*13 did not significantly rescue the lethality (Fig. 5*B*). These data suggest that both variants are loss-of-function alleles: The p.L27P behaves as a mild loss-of-function allele while p.F59Lfs*13 is a strong loss-of-function allele. In addition, the expression of reference TMEM208 rescues the PCP-like defects, whereas expression of the variants only partially rescues the PCP phenotypes (Fig. 5*C*).

Since the patient developed seizures, we tested whether loss of *Tmem208* causes a seizure-like phenotype in $tmem208^{KG4}/Df$ escaper flies. A mechanical stress, caused by a brief vortex stimulation, causes immobility as well as involuntary movements similar to the seizure-like behavior in bang-sensitive flies, whereas the wild-type flies are relatively unaffected by this stimulus (39). We noted minor bang sensitivity in the young mutant flies when compared to control flies (Fig. 5*D*). The bang sensitivity in $Tmem208^{KG4}/Df$ escapers is significantly rescued by the reference transgene, whereas the variants are less effective at rescuing the bang sensitivity (Fig. 5*E*). Although there is no significant difference in rescue ability of the bang sensitivity phenotypes between the reference TMEM208 and p.L27P variant in young flies, when the flies are aged, we observed an increase in bang sensitivity for the flies expressing TMEM208 p.L27P variant (Fig. 5*F*). These data support our observations that the p.L27P acts as a partial loss-of-function variant.

We next focused on determining the mechanism by which the p.L27P variant impacts TMEM208 function. We first assessed the subcellular localization of the reference and variant protein in the wing discs. We did not observe any difference in localization between the reference and p.L27P variant TMEM208 proteins (*SI Appendix*, Fig. S4 *C* and *D*). We also assessed the ER stress levels in the patient-derived fibroblasts. First, we performed RNA-seq on skin fibroblasts from the patient and control and assessed usage of the alternative isoform of *XBP1* with partial exon 4 exclusion, a known marker of ER stress (34). Normalization of the exclusion against the exon 4 to 5 junction present in all *XBP1* isoforms showed that there were a significantly higher proportion of *XBP1* transcripts with partial exon 4 in the patient-derived fibroblasts (UDP11522) compared to control cells (Fig. 5*G*). Additionally, during exposure to thapsigargin, an ER stressor, levels of the protein CHOP (encoded by the human *DDIT3* gene), a transcription factor that is up-regulated with ER stress (40, 41), increased continuously in patient cells during the12-h treatment, unlike control cells (Fig. 5*H*). These data indicate that the patient cells have a decreased ability to respond to ER stress.

## Discussion

*Tmem208* is broadly expressed during fruit fly development, and its loss causes lethality with few escapers. The latter show a reduced

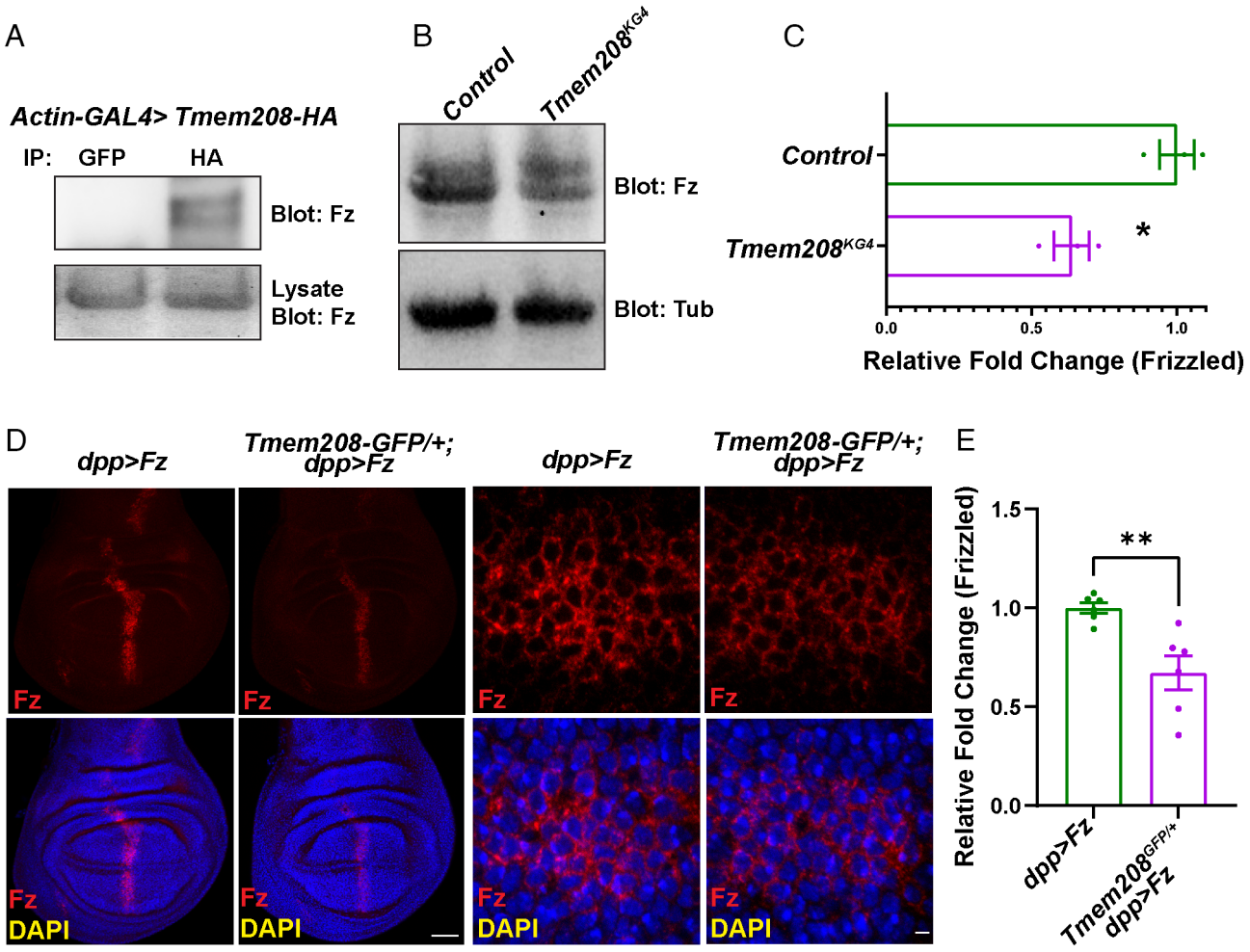


**Fig. 4.** Tmem208 interacts with Fz and helps maintain its levels. (*A*) Western blot from co-IPs showing an interaction between Fz and Tmem208 proteins. (*B* and *C*) Western blot and quantification showing the relative level of Fz protein in *Tmem208*$^{KG4}$ escaper mutant flies. (*D*) Images of wing discs showing the Fz protein levels of the indicated genotypes. Scale bar: 50 μm (lower magnification images) and 2 μm (higher magnification images). The *Lower* panel shows the merged images for Fz and DAPI. (*E*) Relative fold change of Fz protein in the wing discs of the indicated genotypes. To determine the statistical significance between two genotypes, two-tailed Student's *t* test was used. Error bars represent SEM (*$P$ < 0.05; **$P$ < 0.01).

lifespan, seizure-induction-sensitivity, as well as defective leg, eye, and wing development. Our data also revealed cell polarity defects including PCP-like defects in the eyes and wings of flies when *Tmem208* is lost. Consistent with a role of this gene in multicellular development, an individual with compound heterozygous variants in *TMEM208* showed developmental anomalies, dysmorphism, and seizures. We also observe an ER stress response upon loss of *Tmem208*/*TMEM208* in fruit flies and patient cells. Hence, we argue that loss of fly *Tmem208* and its human ortholog impairs development, at least in part, by causing cell polarity and ER defects.

During multicellular growth and development, cell polarity acts at two levels: apicobasal polarity at the cellular level and PCP at the tissue level (37, 42–44). Somatic mutations in apicobasal polarity-related genes typically cause cancers. On the other hand, germline mutations in PCP-related genes cause developmental defects (37, 42, 44, 45). Mutations in PCP pathway genes in humans cause Robinow syndrome and Joubert syndrome, both characterized by a spectrum of symptoms including developmental delay as well as neurological, skeletal, cardiac, and kidney problems (46–51). In mice, loss of PCP leads to developmental defects including abnormal hair pattern formation, as well as cardiac, skeletal, and central nervous system defects (37, 52–57). The transmembrane proteins that help in establishing cell polarity are processed via the ER. Hence, impaired ER function may affect the polarity pathway. The proband with autosomal recessive variants in *TMEM208* displays symptoms that can be related to the phenotypes observed in mice and humans with impaired PCP. These include developmental delay, skeletal, cardiac, and neurological issues, as well as hair patterning defects. Interestingly, the proband also has intercranial hypertension. The CSF inside the brain ventricles moves by synchronized activity of cilia, and the ciliary pattern formation as well as the directional flow of the fluid is regulated by PCP (58–62). Hence, improper beating of the cilia due to abnormal PCP may cause this hypertension.

The proband also presented with seizures. Mutations in PCP-signaling genes, *PRICKLE1* and *PRICKLE2*, have been identified to cause seizures in humans (63). Consistent with these observations, loss of Prickle in mice or flies also causes seizure phenotypes (63) suggesting a connection between PCP and seizure. In summary, the observed PCP defects in mice and humans are consistent with some of the phenotypes observed in the proband. However, the symptoms are relatively mild in the proband probably because of the loss of TMEM208 function is partial and TMEM208$^{L27P}$ likely retains quite a bit of function. It should also be noted that the proband has other symptoms including metabolic issues, microphthalmia, and lymphopenia. Impaired ER homeostasis and up-regulated ER stress cause pathological conditions including metabolic, ocular, and immunological issues (64, 65). Hence, these

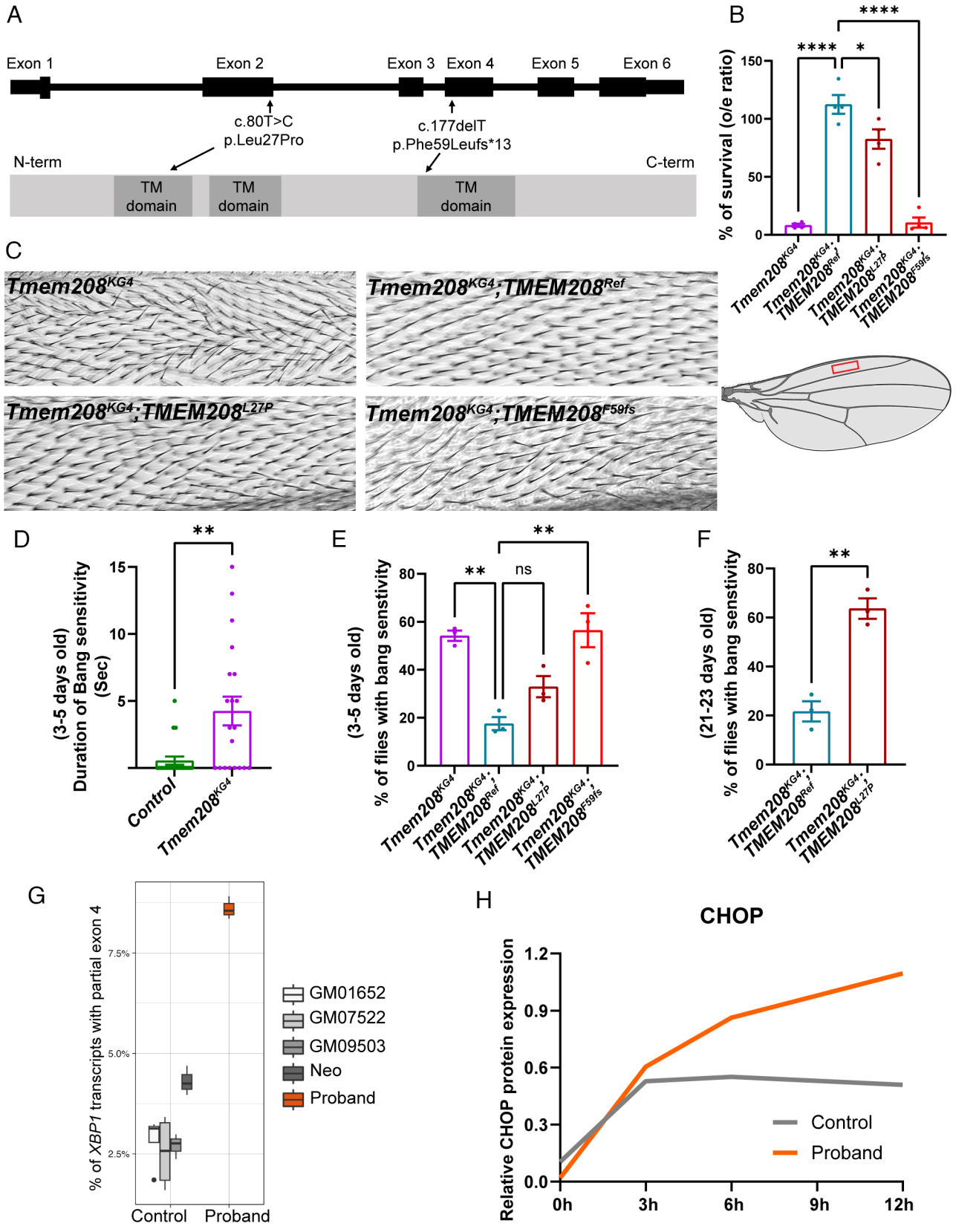


**Fig. 5.** TMEM208 variants are loss of function in nature. (*A*) Schematic of the TMEM208 gene and protein with the relative position of the variants. (*B*) Graph showing the extent of rescue upon expression of human *TMEM208* transgenes. (*C*) Wing images showing the bristle defects and their rescue with human *TMEM208* transgene expression. The area in the red box indicates the region used for the images. The wing image in *C* was drawn using Biorender. (*D*) Duration of bang sensitivity in adult escapers with loss of *Tmem208*. (*E* and *F*) Percentage of flies with the indicated genotypes showing bang sensitivity at two different time points, including young flies at 3 to 5 d old (*E*) and aged flies at 21 to 23 d old (*F*). Error bars represent SEM (*$P < 0.05$; **$P < 0.01$; ****$P < 0.0001$). (*G*) Graph showing the *XBP1* exon 4 usage in fibroblasts from controls and the affected individual. The rate of splicing out part of exon 4 was quantified in each sample (n = 3), normalized against the exon 4 to 5 junction that is present in all isoforms. Differences in exon 4 usage were tested using a 2-sample *t* test. (*H*) Relative CHOP protein levels at different time points upon a 12-h thapsigargin treatment of fibroblasts from unaffected control and affected individual.

additional symptoms in the proband may be due to ER stress that may affect other proteins unrelated to PCP.

Our study also reveals that Tmem208 directly interacts with the PCP pathway protein Fz and helps maintain its levels. Based on previous studies, TMEM208 may target proteins with an internal transmembrane domain (11, 12). Fz harbors multiple internal transmembrane domains (66, 67). It also has an N'-terminal signal peptide (67), which should facilitate its transport via the SRP pathway. Hence, Fz may require both SRP and SND pathways, and loss of Tmem208 may impair the proper dosage of Fz by reducing its translocation to the ER. The mild change of Fz levels and the fact that only mild rotation but no chirality defects are found in *Tmem208* mutant eyes suggest that Tmem208 does not directly affect core PCP functions, but rather may affect PCP effectors including Rho-GTPase family members and Rok or *tricornered*, *fuzzy* (61, 68–70). This is consistent with the notion that the albeit stronger wing hair orientation defects do not show the typical core PCP global effects, but rather local ones. Therefore, it is possible that the levels of some of these effector proteins are impaired due to loss of *Tmem208*, and the partial loss of Fz synergize to cause a PCP-like phenotype. Alternatively, the potential PCP-like phenotypes in the proband can also be linked to ciliary defects.

How does the loss of Tmem208 activate the ER stress response? TMEM208 helps in the import of proteins into the ER, and it also shares substrates with the two other ER protein import pathways, the SRP and GET pathways (11–13, 15, 71). Thus, loss of Tmem208 may affect the import of specific proteins into the ER and activate the Unfolded Protein Response (UPR). Indeed, we noted an elevation of Bip, which is up-regulated upon a UPR (30–32). It is also possible that Tmem208 not only facilitates the translocation of proteins into the ER lumen but also helps in chaperoning nascent proteins in the ER lumen. Finally, an abnormal ER membrane lipid composition, including altered chain length and/or saturation of the fatty acids (72–74), induces a mild ER stress via inositol-requiring enzyme 1 and PKR-like ER Kinase pathways (73, 75, 76), both of which are activated upon loss of *Tmem208*. Further studies are required to investigate whether loss of *Tmem208* affects the composition of ER membrane lipids.

## Materials and Methods

A detailed description of the materials and methods used in this study can be found in *SI Appendix, Supplementary Materials and Methods* and Table S1.

**Fly Stock Maintenance and Longevity Assay.** Fly stocks were maintained in standard cornmeal food medium. The following stocks were used: *UAS-mCherry.NLS w[1118]; Df(2R)Exel7138/CyO* (BL#7883), *w[1118]; Df(2R)BSC308/CyO* (BL#23691), *w[1118]; Dp(2;3)GV-CH321-39L15, PBac{y[+mDint2] w[+mC]=GV-CH321-39L15}VK00031* (BL#89921); *dpp-GAL4:UAS-Fz*; *UAS-Tmem208-HA*; *UAS-Xbp1-EGFP*; *UAS-luci-RNAi*; *UAS-CG8320-RNAi*; *Actin-GAL4*; *Nub-GAL4*. $W^{1118}$ fly strain was used as the *Control*. *UAS-luci-RNAi* was used as the *Control RNAi*. $Tmem208^{KG4}$ in all figures represent the genotype: $Tmem208^{KG4}/Df(2R)Exel7138$. The crosses were performed at 25 °C. RNAi stocks were procured from Vienna Drosophila Stock Center (please see *SI Appendix, Supplementary Material* for details) and the RNAi experiments were performed at 29 °C. Lifespan measurement was carried out at 25 °C as described previously (21). A group of 5 to 6 newly emerged flies were kept together and flipped into a fresh vial every 2 to 3 d until all of the flies were dead. At least 50 flies were tested in each group. The log-rank (Mantel–Cox) test was used to determine the statistical significance.

**Generation of $Tmem208^{KozakGal4}$ and *Tmem208-GFP* Alleles.** $Tmem208^{KozakGal4}/Tmem208^{KG4}$ and *Tmem208-GFP* alleles were generated using CRISPR/Cas9 technology as described previously (18). For the $Tmem208^{KozakGal4}$ line, the coding sequence of *Tmem208* was replaced with *KozakGAL4-3XP3EGFP* cassette using homologous recombination. In Brief, the gRNAs targeting 5′UTR (AGACGTCGCCACGTAAATAGTGG) and the end of the coding region (CGAGTTGGCCTGGTGGTTAAGGG) of *Tmem208* were cloned in pCDF5 vector (Addgene Accession number #73914). A Tmem208-specific plasmid with a restriction cassette, which is flanked on either side by 200-nucleotide homology arms and a gRNA1 target sequence, was synthesized in a pUC57_Kan_gw_OK vector backbone (GENEWIZ, Azenta Life Sciences), and it was used as the homology donor intermediate vector. Subcloning was performed to replace the restriction cassette with an integration cassette that contains *KozakGAL4-polyA-FRT-3XP3- EGFP-FRT*. Subsequently, *yw; iso; attP2(y+){nos-Cas9(v+)}* embryos were injected with 250 ng/μL of the completed plasmid together with pCFD5 vector (100 ng/μL) encoding for the gene-specific sgRNAs. The resulting G0 progenies were crossed to yw flies, and *3XP3-EGFP*-positive flies were selected to establish the stock.

For *Tmem208-GFP* allele, the same homology donor intermediate vector and sgRNAs to generate KozakGAL4 alleles were used to replace the coding region of Tmem208 with the codign region tagged with sfGFP. 3XGGS flexible linker was used in either side of the sfGFP to minimize disruption of the protein structure. Linker-sfGFP-linker is inserted between amino acids R99 and E100. The dominant marker Scarless-DsRed (a gift from O'Conner-Giles lab DGRC# 1364) is inserted at the 3′UTR. Fragments for gene coding region, linker-sfGFP-linker, and Scarless-DsRed were PCR amplified with primers containing overlaps, and the fragments are assembled using the NEB-HiFi DNA Assembly kit (New England Biolabs #E2621) using the manufacturer's instructions, in the homology donor intermediate linearized by BsaI-HF (NEB #R3535). Homology donor vector 250 ng/μL was injected into y w; iso; attP2(y+){nos-Cas9(v+)} embryos, together with pCFD5 vector encoding for the gene-specific sgRNAs (100 ng/μL). The resulting G0 males and females were crossed to *yw* flies to screen for the presence of 3XP3-DsRed.

**Statistical Analyses.** All the statistical analyses were performed using MS Excel and GraphPad Prism (GraphPad Software Inc., CA, USA). For comparing two groups, two-tailed unpaired *t* tests were carried out, and for comparing more than two groups, ANOVA with an appropriate post hoc test were carried out. The results were presented as bar plots where the error bars represent ± SEM. *P*-values of more than 0.05 were considered not significant, whereas *P*-values less than 0.05 were considered significant ($*P < 0.05$, $**P < 0.01$, $***P < 0.001$, and $****P < 0.0001$).

**Data, Materials, and Software Availability.** Some study data are available. An MTA would be required to share human fibroblasts. All other data are included in the article and/or supporting information.

**ACKNOWLEDGMENTS.** We thank the patient and the family for participating in this study. We thank Wen-Wen Lin, Ying Fang, Hongling Pan, and Mei-Chu Huang for fly injections; Dr. H.D.R. for sharing the *UAS-Xbp1-EGFP* stock; and Zongyun Zuo, Guang Lin, Ye-Jin Park, and Matthew Moulton for their technical help. We also extend our thanks to both reviewers for their constructive suggestions. The Intellectual and Developmental Disabilities Research Center confocal microscopy core of Baylor College of Medicine, supported by the National Institute of Child Health & Human Development (U54 HD083092), is duly acknowledged. We thank the Developmental Studies Hybridoma Bank from the University of Iowa for antibodies, as well as Bloomington Drosophila Stock Center, USA, Drosophila Genomics Resource Center (NIH Grant 2P40OD010949), and the Vienna Drosophila Resource Center, Austria for providing cDNA and fly stocks. H.J.B. receives support from the NIH (NINDS and ORIP; R24OD022005, R24OD031447, and U54NS093793), and the Huffington Foundation. H.J.B. is an endowed chair of the Jan and Dan Duncan Neurological Research Institute of Texas Children's Hospital.

1. T. Wrzesiński *et al.*, Expression of pre-selected TMEMs with predicted ER localization as potential classifiers of ccRCC tumors. *BMC Cancer* **15**, 518 (2015).
2. K. Schmit, C. Michiels, TMEM proteins in cancer: A review. *Front. Pharmacol.* **9**, 1345 (2018).
3. M. C. Do Rosario *et al.*, Variants in the zinc transporter TMEM163 cause a hypomyelinating leukodystrophy. *Brain* **145**, 4202–4209 (2022).
4. J. Stephen *et al.*, Bi-allelic TMEM94 truncating variants are associated with neurodevelopmental delay, congenital heart defects, and distinct facial dysmorphism. *Am. J. Hum. Genet.* **103**, 948–967 (2018).
5. C. Y. Li *et al.*, Mutation analysis of TMEM family members for early-onset Parkinson's disease in Chinese population. *Neurobiol. Aging* **101**, 299.e1–299.e6 (2021).

6. Y. Zhao *et al.*, Genetic analysis of six transmembrane protein family genes in Parkinson's disease in a large chinese cohort. *Front. Aging Neurosci.* **14**, 889057 (2022).
7. A. Ta-Shma *et al.*, Mutations in TMEM260 cause a pediatric neurodevelopmental, cardiac, and renal syndrome. *Am. J. Hum. Genet.* **100**, 666–675 (2017).
8. D. L. Polla *et al.*, Biallelic variants in TMEM222 cause a new autosomal recessive neurodevelopmental disorder. *Genet. Med.* **23**, 1246–1254 (2021).
9. J. C. Jansen *et al.*, TMEM199 deficiency is a disorder of golgi homeostasis characterized by elevated aminotransferases, alkaline phosphatase, and cholesterol and abnormal glycosylation. *Am. J. Hum. Genet.* **98**, 322–330 (2016).
10. Q. Thomas *et al.*, Bi-allelic loss-of-function variants in TMEM147 cause moderate to profound intellectual disability with facial dysmorphism and pseudo-Pelger-Huët anomaly. *Am. J. Hum. Genet.* **109**, 1909–1922 (2022).
11. N. Aviram *et al.*, The SND proteins constitute an alternative targeting route to the endoplasmic reticulum. *Nature* **540**, 134–138 (2016).
12. S. Haßdenteufel *et al.*, hSnd2 protein represents an alternative targeting factor to the endoplasmic reticulum in human cells. *FEBS Lett.* **591**, 3211–3224 (2017).
13. A. Tirincsi, M. Sicking, D. Hadzibeganovic, S. Haßdenteufel, S. Lang, The molecular biodiversity of protein targeting and protein transport related to the endoplasmic reticulum. *Int. J. Mol. Sci.* **23**, 143 (2022).
14. M. R. Pool, Targeting of proteins for translocation at the endoplasmic reticulum. *Int. J. Mol. Sci.* **23**, 3773 (2022).
15. J. Casson *et al.*, Multiple pathways facilitate the biogenesis of mammalian tail-anchored proteins. *J. Cell Sci.* **130**, 3851–3861 (2017).
16. Y. Hu *et al.*, An integrative approach to ortholog prediction for disease-focused and other functional studies. *BMC Bioinf.* **12**, 357 (2011).
17. A. H. Brand, N. Perrimon, Targeted gene expression as a means of altering cell fates and generating dominant phenotypes. *Development* **118**, 401–415 (1993).
18. O. Kanca *et al.*, An expanded toolkit for Drosophila gene tagging using synthesized homology donor constructs for CRISPR-mediated homologous recombination. *Elife* **11**, e76077 (2022).
19. P. T. Lee *et al.*, A gene-specific T2A-GAL4 library for drosophila. *Elife* **7**, e35574 (2018).
20. S. Nagarkar-Jaiswal *et al.*, A genetic toolkit for tagging intronic MiMIC containing genes. *Elife* **4**, 2–9 (2015).
21. D. Dutta *et al.*, A defect in mitochondrial fatty acid synthesis impairs iron metabolism and causes elevated ceramide levels. *Nat. Metab.* **5**, 1595–1614 (2023).
22. K. J. T. Venken *et al.*, Versatile P[acman] BAC libraries for transgenesis studies in Drosophila melanogaster. *Nat. Methods* **6**, 431–434 (2009).
23. J. E. Treisman, Retinal differentiation in Drosophila. *Wiley Interdiscip. Rev. Dev. Biol.* **2**, 545–557 (2013).
24. N. Pinal *et al.*, Regulated and polarized PtdIns(3,4,5)P3 accumulation is essential for apical membrane morphogenesis in photoreceptor epithelial cells. *Curr. Biol.* **16**, 140–149 (2006).
25. F. Pichaud, PAR-Complex and crumbs function during photoreceptor morphogenesis and retinal degeneration. *Front. Cell. Neurosci.* **12**, 1–9 (2018).
26. U. Tepass, K. P. Harris, Adherens junctions in Drosophila retinal morphogenesis. *Trends Cell Biol.* **17**, 26–35 (2007).
27. M. Pellikka *et al.*, Crumbs, the Drosophila homologue of human CRB1/RP12, is essential for photoreceptor morphogenesis. *Nature* **416**, 143–149 (2002).
28. Y. Hong, L. Ackerman, L. Y. Jan, Y. N. Jan, Distinct roles of Bazooka and Stardust in the specification of Drosophila photoreceptor membrane architecture. *Proc. Natl. Acad. Sci. U.S.A.* **100**, 12712–12717 (2003).
29. Y. Zhao *et al.*, Transmembrane protein 208: A novel ER-Localized protein that regulates autophagy and ER stress. *PLoS One* **8**, e64228 (2013).
30. C. Hetz, The unfolded protein response: Controlling cell fate decisions under ER stress and beyond. *Nat. Rev. Mol. Cell Biol.* **13**, 89–102 (2012).
31. R. Costa *et al.*, Impaired mitochondrial ATP production downregulates Wnt signaling via ER stress induction. *Cell Rep.* **28**, 1949–1960.e6 (2019).
32. H. D. Ryoo, P. M. Domingos, M. J. Kang, H. Steller, Unfolded protein response in a Drosophila model for retinal degeneration. *EMBO J.* **26**, 242–252 (2007).
33. M. Şentürk *et al.*, Ubiquilins regulate autophagic flux through mTOR signalling and lysosomal acidification. *Nat. Cell Biol.* **21**, 384–396 (2019).
34. H. Yoshida, T. Matsui, A. Yamamoto, T. Okada, K. Mori, XBP1 mRNA is induced by ATF6 and spliced by IRE1 in response to ER stress to produce a highly active transcription factor. *Cell* **107**, 881–891 (2001).
35. M. Sone, X. Zeng, J. Larese, H. D. Ryoo, A modified UPR stress sensing system reveals a novel tissue distribution of IRE1/XBP1 activity during normal Drosophila development. *Cell Stress Chaperones* **18**, 307–319 (2013).
36. C. Harrison, H. Shao, H. Strutt, D. Strutt, Molecular mechanisms mediating asymmetric subcellular localisation of the core planar polarity pathway proteins. *Biochem. Soc. Trans.* **48**, 1297–1308 (2020).
37. M. Simons, M. Mlodzik, Planar cell polarity signaling: From fly development to human disease. *Annu. Rev. Genet.* **42**, 517–540 (2008).
38. J. Wang *et al.*, MARRVEL: Integration of human and model organism genetic resources to facilitate functional annotation of the human genome. *Am. J. Hum. Genet.* **100**, 843–853 (2017).
39. J. Mituzaite, R. Petersen, A. Claridge-Chang, R. A. Baines, Characterization of seizure induction methods in drosophila. *eNeuro* **8**, ENEURO.0079-21 (2021).
40. S. Oyadomari, M. Mori, Roles of CHOP/GADD153 in endoplasmic reticulum stress. *Cell Death Differ.* **11**, 381–389 (2004).
41. H. Nishitoh, CHOP is a multifunctional transcription factor in the ER stress response. *J. Biochem.* **151**, 217–219 (2012).
42. P. Lo, H. Hawrot, M. Georgiou, Apicobasal polarity and its role in cancer progression. *Biomol. Concepts* **3**, 505–521 (2012).
43. C. E. Buckley, D. St Johnston, Apical–basal polarity and the control of epithelial form and function. *Nat. Rev. Mol. Cell Biol.* **23**, 559–577 (2022).
44. L. V. Goodrich, D. Strutt, Principles of planar polarity in animal development. *Development* **138**, 1877–1892 (2011).
45. M. Lee, V. Vasioukhin, Cell polarity and cancer–Cell and tissue polarity as a non-canonical tumor suppressor. *J. Cell Sci.* **121**, 1141–1150 (2008).
46. E. McPherson, C. Zaleski, P. F. Giampietro, Robinow syndrome with variable neurologic features. *Genet. Med.* **8**, 59–60 (2006).
47. R. Bachmann-Gagescu *et al.*, Joubert syndrome: A model for untangling recessive disorders with extreme genetic heterogeneity. *J. Med. Genet.* **52**, 514–522 (2015).
48. F. Brancati, B. Dallapiccola, E. M. Valente, Joubert Syndrome and related disorders. *Orphanet J. Rare Dis.* **5**, 20 (2010).
49. A. M. Wabik *et al.*, Nephrological and urological symptoms in patients with Robinow syndrome–A report of two cases. *Pol. Merkur. Lekarski* **50**, 302–305 (2022).
50. M. G. Butler, W. B. Wadlington, Robinow syndrome: Report of two patients and review of literature. *Clin. Genet.* **31**, 77–85 (1987).
51. M. Barzegar, M. Malaki, E. Sadegi-Hokmabadi, Joubert syndrome with variable features: Presentation of two cases. *Iran J. Child Neurol.* **7**, 43–46 (2013).
52. H. Brzóska *et al.*, Planar cell polarity genes Celsr1 and Vangl2 are necessary for kidney growth, differentiation, and rostrocaudal patterning. *Kidney Int.* **90**, 1274–1284 (2016).
53. M. Cetera, L. Leybova, F. W. Woo, M. Deans, D. Devenport, Planar cell polarity-dependent and independent functions in the emergence of tissue-scale hair follicle patterns. *Dev. Biol.* **428**, 188–203 (2017).
54. S. A. Ramsbottom *et al.*, Vangl2-Regulated polarisation of second heart field-derived cells is required for outflow tract lengthening during cardiac development. *PLoS Genet.* **10**, e1004871 (2014).
55. J. N. Murdoch *et al.*, Genetic interactions between planar cell polarity genes cause diverse neural tube defects in mice. *DMM Dis. Model. Mech.* **7**, 1153–1163 (2014).
56. B. Wang, T. Sinha, K. Jiao, R. Serra, J. Wang, Disruption of PCP signaling causes limb morphogenesis and skeletal defects and may underlie Robinow syndrome and brachydactyly type B. *Hum. Mol. Genet.* **20**, 271–285 (2011).
57. N. Guo, C. Hawkins, J. Nathans, Frizzled6 controls hair patterning in mice. *PNAS* **101**, 9277–9281 (2004).
58. G. Eichele *et al.*, Cilia-driven flows in the brain third ventricle. *Philos. Trans. R. Soc. B Biol. Sci.* **375**, 20190154 (2020).
59. R. Faubel, C. Westendorf, E. Bodenschatz, G. Eichele, Cilia-based flow network in the brain ventricles. *Science* **353**, 176–178 (2016).
60. M. T. Butler, J. B. Wallingford, Planar cell polarity in development and disease. *Nat. Rev. Mol. Cell Biol.* **18**, 375–388 (2017).
61. J. B. Wallingford, Planar cell polarity signaling, cilia and polarized ciliary beating. *Curr. Opin. Cell Biol.* **22**, 597–604 (2010).
62. D. H. Kelley, J. H. Thomas, Cerebrospinal fluid flow. *Annu. Rev. Fluid Mech.* **55**, 237–264 (2023).
63. H. Tao *et al.*, Mutations in prickle orthologs cause seizures in flies, mice, and humans. *Am. J. Hum. Genet.* **88**, 138–149 (2011).
64. C. Hetz, K. Zhang, R. J. Kaufman, Mechanisms, regulation and functions of the unfolded protein response. *Nat. Rev. Mol. Cell Biol.* **21**, 421–438 (2020).
65. H. Kroeger, W. C. Chiang, J. Felden, A. Nguyen, J. H. Lin, ER stress and unfolded protein response in ocular health and disease. *FEBS J.* **286**, 399–412 (2019).
66. R. E. Krasnow, P. N. Adler, A single frizzled protein has a dual function in tissue polarity. *Development* **120**, 1883–1893 (1994).
67. H.-C. Huang, P. S. Klein, The Frizzled family: Receptors for multiple signal transduction pathways Gene organization and evolutionary history Characteristic structural features. *Genome Biol.* **5**, 1–7 (2004).
68. Y. Koca, G. M. Collu, M. Mlodzik, *Wnt-Frizzled Planar Cell Polarity Signaling in the Regulation of Cell Motility* (Elsevier Inc., ed. 1, 2022).
69. J. R. K. Seifert, M. Mlodzik, Frizzled/PCP signalling: A conserved mechanism regulating cell polarity and directed motility. *Nat. Rev. Genet.* **8**, 126–138 (2007).
70. C. G. Winter *et al.*, Drosophila Rho-associated kinase (Drok) links Frizzled-mediated planar cell polarity signaling to the actin cytoskeleton. *Cell* **105**, 81–91 (2001).
71. J. Yang *et al.*, Human SND2 mediates ER targeting of GPI-anchored proteins with low hydrophobic GPI attachment signals. *FEBS Lett.* **595**, 1542–1558 (2021).
72. K. Halbleib *et al.*, Activation of the unfolded protein response by lipid bilayer stress. *Mol. Cell* **67**, 673–684 (2017).
73. R. Volmer, D. Ron, Lipid-dependent regulation of the unfolded protein response. *Curr. Opin. Cell Biol.* **33**, 67–73 (2015).
74. G. Thibault *et al.*, The membrane stress response buffers lethal effects of lipid disequilibrium by reprogramming the protein homeostasis network. *Mol. Cell* **48**, 16–27 (2012).
75. R. Volmer, K. Van Der Ploeg, D. Ron, Membrane lipid saturation activates endoplasmic reticulum unfolded protein response transducers through their transmembrane domains. *Proc. Natl. Acad. Sci. U.S.A.* **110**, 4628–4633 (2013).
76. N. Kono, N. Amin-Wetzel, D. Ron, Generic membrane-spanning features endow IRE1α with responsiveness to membrane aberrancy. *Mol. Biol. Cell* **28**, 2318–2332 (2017).